Applied Organometallic Chemistry (1987) 1 545–554
© Longman Group UK Ltd 1987

02682605/87/01608545/$03.50

Kinetic studies on the reaction of methylcobalamin with metal oxides

John S Thayer
Department of Chemistry, University of Cincinnati, Cincinnati, Ohio 45221, USA

Received 17 March 1987 Accepted 30 September 1987

Aqueous solutions of methylcobalamin (CH_3B_{12}) react with various water-insoluble metal oxides. The decomposition of methylcobalamin follows a kinetic pattern of two parallel first-order reactions. A proposed reaction mechanism involves the attachment of methylcobalamin to the oxide surface, followed by methyl transfer and dissolution of the oxide.

Keywords: Methylcobalamin (CH_3B_{12}), metal oxides, methyl transfer, solid-surface reactions, metal oxide dissolution

INTRODUCTION

Methylcobalamin (CH_3B_{12}) plays a crucial role in the biological methylation of metals by bacteria.[1] Methyl transfer reactions between this compound and a variety of metal substrates have been investigated, and extensive kinetic data have been accumulated.[2] These investigations have been concentrated almost exclusively on homogeneous systems. Corresponding investigations on heterogeneous systems have been infrequent. In the presence of excess solid sodium bismuthate ($NaBiO_3$) or phenylmercuric acetate ($C_6H_5HgC_2H_3O_2$) the rate of decomposition of CH_3B_{12} rose linearly with increasing quantity of solid.[3] Lead dioxide and platinum dioxide reacted with this compound.[4] Kinetic studies showed that the rate of disappearance of CH_3B_{12} in the presence of solid lead dioxide followed a kinetic pattern of two parallel first-order reactions.[5]

We have found that a number of other metal oxides also cause demethylation of CH_3B_{12}, and that this demethylation likewise follows the pattern of two parallel first-order reactions. This paper will present our results and a proposed mechanism.

EXPERIMENTAL

Reagents

The metal oxides for these experiments were purchased from commercial sources and used as such. In addition, lead dioxide and thallium(III) oxide were prepared by hydrolysis of the corresponding acetates, which were obtained from commercial sources. When particle size studies were required, the oxides were passed through various sieves ranging from ASTM #20 mesh (850 μm) to ASTM #400 mesh (38 μm) by shaking on a Gilson SS-15 shaker for 15 to 30 min. Methylcobalamin was purchased from Sigma Chemical Company and kept in the dark at -10°C until needed. Other inorganic salts or reagents used were obtained from commercial sources and not further purified.

Experimental procedures

Solutions of methylcobalamin (10^{-3}–10^{-5} mol dm^{-3}) in 0.10 mol dm^{-3} acetic acid–0.10 mol dm^{-3} sodium acetate were prepared immediately before use. The more reactive oxides ($k_2 > 10^{-4}$ s^{-1}) were treated in a cuvette in the presence of 3.0–3.3 cm^3 solution and monitored directly by UV–visible spectroscopy, especially at 350 nm ($H_2OCoB_{12}{}^+$). Less reactive oxides were reacted in test tubes with 20–25 cm^3 solution; these were kept in the dark for the duration of the run, with small aliquots being periodically removed for spectroscopic analysis.

Instrumental studies

Kinetic studies were performed on a Cary 14 recording UV–visible spectrophotometer (UV) using techniques elsewhere described.[6] Atomic absorption (AA) spectrometric investigations utilized either a Unicam SP-90 or a Perkin–Elmer Model 460 atomic absorption spectrophotometer, using hollow cathode lamps. Calibration solutions were freshly prepared before each run. Chromatographic investigations utilized a Hewlett–Packard Model 5730 dual-column vapor-phase chromatograph (GC) with a 2 m glass column containing DEGS packing and a HP18710A Flame Ionization Detector. Nitrogen was used as a carier gas, and the column temperature was maintained at 50°C. Product studies were also carried out using a quartz furnace GCAA system whose details are presented elsewhere.[7] Peaks were identified by comparison of retention times with known standards, occasionally including 'spiking'. Experimentally determined points were fitted to lines using the APPLESTAT® program and an Apple IIe® computer; slopes, intercepts and correlation coefficients were also calculated using this program.

RESULTS

Kinetic experiments

The reaction between CH_3B_{12} and silver(II) oxide follows the kinetic plot pattern shown in Fig. 1. Following the nomenclature of Moore and Pearson,[8] we have used k_2 and k_1 to indicate the rate constants for the faster and slower reactions respectively, with A_0 and B_0 representing the initial concentrations of CH_3B_{12} disappearing by each pathway. The sum A_0+B_0 is the total starting CH_3B_{12} concentration. Table 1 lists the experimentally determined reaction rate constants. Correlation coefficients for each individual experiment ranged from 0.910 to 0.999, with the faster-reacting oxides giving the better correlation. The total extent of reaction varied from system to system, but rarely went to completion, even at oxide/CH_3B_{12} ratios of 1000:1.

Parameter variations

For any specific metal oxide, the experimental values for k_2 and k_1 showed little variation from one system to another. By contrast, the two concentration terms, A_0 and B_0, showed much more dependence on specific reaction parameters. For this reason, we found the ratio $A_0/(A_0+B_0)$, representing the proportion of reaction proceed-

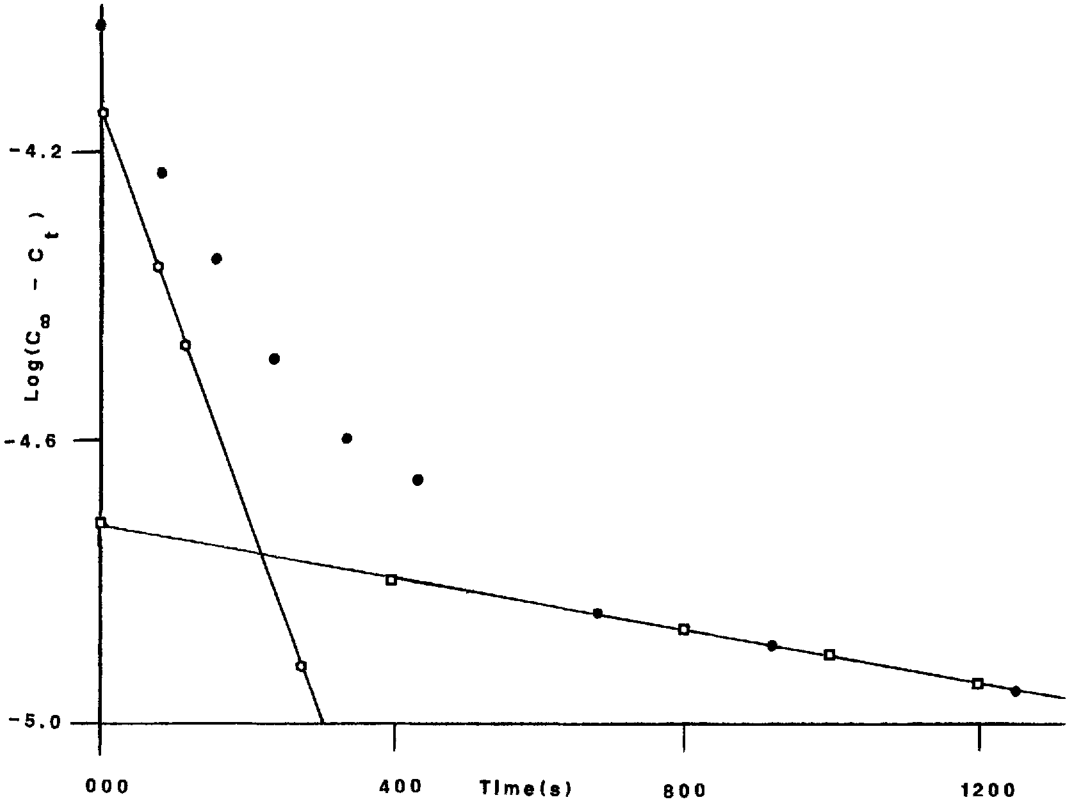

Figure 1 Kinetics plot of the reaction of 9.35×10^{-5} mol dm^{-3} CH_3B_{12} with AgO. Solid circles represent experimental points; open symbols represent calculated points.

Table 1 Experimentally determined rate constants for metal oxide–methylcobalamin reactions

Metal oxide	No. of expts	k_2[S.D.[a]] (s^{-1})	k_1[S.D.] (s^{-1})
Ni_2O_3	8	$5.82[0.63] \times 10^{-3}$	$5.74[0.94] \times 10^{-4}$
AgO	6	$4.72[0.96] \times 10^{-3}$	$1.79[0.29] \times 10^{-4}$
NiO_2	7	$3.13[0.62] \times 10^{-3}$	$3.17[0.72] \times 10^{-4}$
Tl_2O_3	9	$2.35[0.66] \times 10^{-3}$	$1.27[0.44] \times 10^{-4}$
PbO_2[b]	10	$1.02[0.14] \times 10^{-3}$	$5.33[0.85] \times 10^{-5}$
$NaBiO_3$	6	$3.12[0.46] \times 10^{-4}$	$2.23[0.46] \times 10^{-6}$
Pb_3O_4	6	$2.36[0.62] \times 10^{-5}$	$7.47[0.74] \times 10^{-7}$
Mn_3O_4	9	$2.04[0.35] \times 10^{-5}$	$1.88[0.40] \times 10^{-7}$
MnO_2	11	$1.02[0.24] \times 10^{-5}$	$1.15[0.19] \times 10^{-7}$
Mn_2O_3	9	$7.36[0.84] \times 10^{-6}$	$1.62[0.31] \times 10^{-7}$
Ag_2O	6	$3.27[0.73] \times 10^{-6}$	$1.21[0.21] \times 10^{-8}$

[a] S.D., standard deviation. [b] Ref. 5.

ing by the faster pathway, to be a useful parameter for making inter-system comparisons. When the total quantity of CH_3B_{12} was held constant and the quantity of solid metal oxide increased, the proportion $A_0/(A_0+B_0)$ also increased[5] (see Table 2). If the quantities of both metal oxide and CH_3B_{12} were fixed and only the particle size range of the oxide varied, the proportion of the faster pathway increased as the particle size decreased (Table 2).

As reported previously,[5] reactivity of lead(IV) dioxide (PbO_2) towards CH_3B_{12} decreased as the pH and/or the acetate ion concentration decreased. This also seems to be true for other metal oxides. Also, when extra quantities of a salt containing the metal in a less positive (i.e. lower) oxidiation state (e.g. $Mn(NO_3)_2$ for MnO_2 or Mn_2O_3; $Pb(NO_3)_2$ for PbO_2, etc.) were added to a reaction system, the ratio $A_0/(A_0+B_0)$ decreased (Table 3).

The presence of surface groups almost certainly is important. Lead(IV) oxide and thallium(III) oxide (Tl_2O_3) prepared by hydrolysis of the corresponding acetates (and therefore probably having some residual acetate groups) reacted considerably more rapidly with CH_3B_{12} than did corresponding quantities of the oxides obtained from commercial sources.

Product analysis

Spectroscopic evidence has indicated that aquocobalamin was the only corrinoid product to be formed when lead(IV) oxide reacted with methylcobalamin;[5] the methyl groups formed a variety of volatile organic molecules (methane, ethane, methanol, acetone, etc.), and traces of tetramethyllead could be detected.[5] Treatment of tin(IV) oxide (SnO_2) with methylcobalamin led to

Table 2 Solid substrate parameters

Variation in total quantity of substrate (Pb_3O_4)[a]

(μmol) oxide	Reaction (%)	A_0(mol dm^{-3}, $\times 10^4$)	B_0(mol dm^{-3}, $\times 10^4$)	$A_0/(A_0+B_0)$
36.5	40.0	0.24	2.39	0.091
146.7	52.2	0.60	2.02	0.229
298.1	53.0	0.63	1.99	0.240
667.6	72.2	1.16	1.47	0.441

Variation in substrate particle size (Mn_3O_4)[b]

Particle size range (μm)	Reaction (%)	A_0(mol dm^{-3}, $\times 10^5$)	B_0(mol dm^{-3}, $\times 10^5$)	$A_0/(A_0+B_0)$
425–850	36.3	1.87	3.75	0.245
250–425	53.6	2.26	5.36	0.297
150–250	56.4	2.50	5.12	0.328

[a] Each system used 20.0 cm^3 of 2.62×10^{-4} mol dm^{-3} (5.24 μmol) CH_3B_{12} in buffered acetic acid. (For product analysis see Ref. 5).

[b] Each system used 3319 ± 26 μmol oxide and 20.0 cm^3 of 7.62×10^{-5} mol dm^{-3} (1.52 μmol) CH_3B_{12} in buffered acetic acid.

Table 3 Product salt effects

Compound	Quantity (mmol)	CH_3B_{12} (mol dm^{-3})	A_0(mol dm^{-3})	B_0(mol dm^{-3})	$A_0/(A_0+B_0)$
PbO_2	3.121+0	4.46×10^{-5}	1.46	3.00	0.327
$PbO_2/Pb(NO_3)_2$	3.181+3.119		1.28	3.18	0.287
Mn_3O_4	3.972+0	1.51×10^{-4}	0.41	1.10	0.272
$Mn_3O_4/Mn(C_2H_3O_2)_2$	3.972+0.495		0.21	1.30	0.139
Pb_3O_4	1.521+0	1.39×10^{-4}	0.957	0.433	0.688
$Pb_3O_4/Pb(NO_3)_2$	1.521+1.256		0.517	0.873	0.372
Ni_2O_3	2.070+0	5.58×10^{-5}	2.76	2.82	0.495
$Ni_2O_3/Ni(NO_3)_2$	2.070+0.123		1.70	3.88	0.305

formation of methyltin products detectable by GCAA (Fig. 2), although the reaction was too slow for convenient kinetics measurement. Other metal oxides formed volatile products consistent with the transient existence of methylmetal intermediates. Ethane was the predominant product in the reaction of CH_3B_{12} with silver(II) oxide ($Ag^IAg^{III}O_2$, giving Ag^{II} in acid solution), and with nickel(III) oxide [NiO(OH)]. The reaction between CH_3B_{12} and silver(I) oxide (Ag_2O) left a ring of metallic silver on the inner surface of the reaction vessel; such a ring did not form in the absence of CH_3B_{12}. Bright orange redlead oxide (Pb_3O_4) solid had a black coating [probably PbO + lead(0)] after reaction with CH_3B_{12}. Analyses using atomic absorption spectrophotometry (AA) of the reaction solutions indicated that the presence of CH_3B_{12} increased the quantity of dissolved metal very substantially; some selected examples appear in Table 4.

Other oxides

Various metal oxides in addition to those reported in Table 1 were examined for their reactivity towards CH_3B_{12} (see also the Appendix). In agreement with an earlier report,[4] we found that platinum(IV) oxide reacted readily with methylcobalamin, but were unable to get consistent, reproducible kinetic results. Mercury(II) oxide (HgO) dissolved too extensively and reacted too readily to yield good data. Most other metal oxides tested reacted too slowly or too slightly for reproducible results; these include tin(IV) oxide (SnO_2), antimony(V) oxide (Sb_2O_5), bismuth(III) oxide (Bi_2O_3), indium(III) oxide (In_2O_3), titanium(IV) oxide (TiO_2), germanium(IV) oxide (GeO_2) and thorium(IV) oxide (ThO_2). Certain oxides showed no reactivity at all towards CH_3B_{12} (defined as no change in the absorbance at 350 nm after one week in the dark); these include gallium(III) oxide (Ga_2O_3), zirconium(IV) oxide (ZrO_2) and iron(III) oxide (Fe_2O_3). Rather unexpectedly, cerium(IV) oxide (CeO_2) did not react, nor did calcium peroxide (CaO_2). These latter constitute *de facto* control reactions for CH_3B_{12}.

DISCUSSION

Kinetics model

For the faster reaction in the PbO_2–CH_3B_{12} system, we proposed a mechanism involving at-

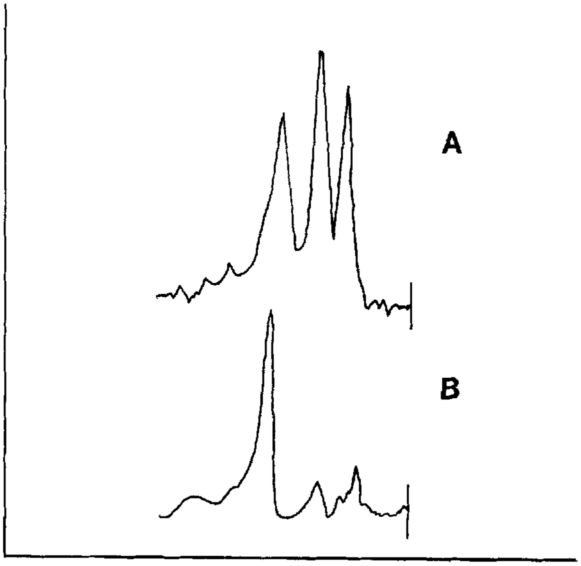

Figure 2 GC trace (with AA detection)[13] of hydride-generated products of SnO_2–CH_3B_{12} system. Trace A shows (left to right) $(CH_3)_3SnH$, $(CH_3)_2SnH_2$ and CH_3SnH_3 from standard solution. Trace B shows hydride-generated products of the reaction. (Time increases right to left.)

Table 4 Enhancement of metal dissolution by methylcobalamin[a]

Metal oxide	Time (s) × 10^3	Reaction	Control	Enhancement (fold)
PbO_2	4.20	91.0	6.5	14.0
$NaBiO_3$	33.4	21.0	2.1	10.0
MnO_2	243.7	54.0	19.0	2.84
PtO_2	691.2	19.3	9.0	2.14

[a]All systems run in buffered acetic acid. Concentrations – mg dm^{-3}. Oxides that did *not* react with CH_3B_{12} represent a blank control for enhancement of metal dissolution effects (e.g. CeO_2, CaO_2).

tachment of CH_3B_{12} to the oxide surface, followed by methyl transfer and dissolution.[5] Using the model proposed by Stone and Morgan[9] for the reaction of hydroquinone with manganese oxides, assuming an equilibrium between bound and dissolved CH_3B_{12}, and designating a metal site as $O_nM—$, we can write the following equations (charges not shown):

$$O_nM—_{(s)} + CH_3B_{12(aq)} \overset{K_{eq}}{\rightleftharpoons} O_nM—CH_3B_{12(s)} \quad [1]$$

$$O_nM—CH_3B_{12(s)} + H_2O_{(l)} \xrightarrow{k_2} M—CH_{3(aq)} + H_2OB_{12(aq)} \quad [2]$$

From these equations can be derived the rate expressions:

$$\frac{d[M—CH_3]}{dt} = k_2[O_nM—CH_3B_{12}] \quad [3]$$

and

$$\frac{d[O_nM—CH_3B_{12}]}{dt} = K_{eq}[CH_3B_{12}]\,[O_nM—] - k_2[O_nM—CH_3B_{12}] \quad [4]$$

If S_T is used to designate the total number of binding sites, bound or unoccupied, on the metal oxide surface, then:

$$S_T = [O_nM—] + [O_nM—CH_3B_{12}] \quad [5]$$

and Eqn [4] may be rewritten as

$$\frac{d[O_nM—CH_3B_{12}]}{dt} = K_{eq}S_T[CH_3B_{12}] - (K_{eq}[CH_3B_{12}] + k_2)[O_nM—CH_3B_{12}] \quad [6]$$

Assuming that $[O_nM—CH_3B_{12}]$ is constant (a 'steady-state' approximation), then

$$\frac{d}{dt}[O_nM—CH_3B_{12}] = 0$$

and Eqn [6] becomes:

$$\frac{d[M—CH_3]}{dt} = \frac{K_{eq}k_2S_T[CH_3B_{12}]}{K_{eq}[CH_3B_{12}]+1}. \quad [7]$$

Due to the very high optical density of the absorption peak at 350 nm in CH_3B_{12}, our solutions usually involved concentrations of 10^{-3} mol dm^{-3} or lower. Our observations indicated that addition of metal oxide caused little immediate decrease in CH_3B_{12} 350 nm absorbance.[10] This suggests that the term $K_{eq}[CH_3B_{12}]$ may be considerably less than unity, which in turn would make Eqn [7] a first-order rate expression.

Mechanism

We propose that the reaction between metal oxides and CH_3B_{12} involves two *parallel* first-order processes: a surface reaction (Eqns [1] and [2]) for the faster process and a solution reaction for the slower process. The relative importance of the two processes changes as factors affecting the surface area change; an increase in the surface area of the solid oxide increases the proportion of CH_3B_{12} decomposing by the faster pathway. The suppressive effect of product salts may be explained if one assumes that the salt ion in solution is competing with CH_3B_{12} for attachment at a surface binding site. Whether this attachment causes destruction of the site, or merely results in reversible blockage, the effective value of S_T in Eqn [5] is lowered, thereby reducing the rate of reaction. The lack of reaction between calcium peroxide and CH_3B_{12} suggests that the metal atom itself serves as the crucial site, as does the observation of tetramethyllead among the products of the PbO_2–CH_3B_{12} reaction.[5] If the methyl group undergoes transfer to an electrophilic metal atom (as proposed elsewhere[2]), then anything enhancing the electrophilic nature of the metal atom should enhance the reaction with CH_3B_{12}. The most reactive metal oxides are good oxidizing agents, such as nickel(III) oxide, silver(II) oxide, etc. Those metals that form oxides in two or more oxidation states generally show little or no reactivity towards CH_3B_{12} in the lower states. Other factors, presently unknown, may also be involved.

We proposed that the slower reaction in the case of lead(IV) oxide might be a solution reaction between CH_3B_{12} and a low, steadily replenished, concentration of dissolved lead arising from the solid dioxide.[5] A saturated solution of sodium bismuthate reacted with CH_3B_{12} even in the absence of extra solid.[3] Thallium(III) acetate dissolved in buffered acetic acid reacted with CH_3B_{12} following second-order kinetics,[11] with a rate constant of $72.3\,\mathrm{dm^3\,mol^{-1}\,s^{-1}}$. If one assumes that thallium(III) oxide dissolved in buffered acetic acid forms the same reactive species as thallium(III) acetate (possibly $Tl(C_2H_3O_2)_2^+$), then k_2 may be considered a pseudo-first order rate constant, and the concentration of dissolved) thallium(III) may be estimated as $1.27\times10^{-4}\,\mathrm{s^{-1}}/72.3\,\mathrm{dm^3\,mol^{-1}\,s^{-1}} = 1.75\times10^{-6}\,\mathrm{mol\,dm^{-3}}$. This value is much lower than any CH_3B_{12} concentration we have used. While this does not prove our assumption, it is at least consistent with it.

CONCLUSIONS

A variety of water-insoluble metal oxides react with methylcobalamin in buffered acetic acid. The reagent decomposes by a kinetic pattern of two parallel first-order reactions, whose relative importance can be altered by changing the reaction conditions. The faster reaction may occur through attachment at the oxide surface, while the slower reaction may be a solution reaction.

Methylcobalamin within organisms is attached to proteins.[12] Presumably then, intracellular biological methylation involving this compound would follow typical enzyme kinetic patterns rather than patterns observed for CH_3B_{12}–metal solutions.[1,2] Methylation in environmental waters need not be restricted to intracellular methylation; there is some evidence that extracellular methylation may also occur.[1,2] These metal oxides–methylcobalamin systems may provide useful information on how such extracellular methylation might occur and possibly serve as useful models. Investigations into all aspects of these reactions are continuing.

Acknowledgements The author wishes to thank Dr F E Brinckman (National Bureau of Standards) for the use of the atomic absorption spectrophotometers and the gas chromatograph and for helpful discussions. The author also wishes to thank Dr G J Olson (NBS), Mr W R Blair (NBS) and Dr T W Brueggemeyer (UC) for their technical assistance at various points in this project, and gratefully acknowledges a University Research Council grant from the University of Cincinnati that helped to support this work. GCAA data was obtained by the author at Leicester Polytechnic, UK.

REFERENCES

1. Thayer, J S *Organometallic Compounds and Living Organisms*, Academic Press, New York, 1984
2. Thayer, J S and Brinckman, F E *Ad. Organomet. Chem.*, 1982, 20: 313
3. Thayer, J S In: *Proceedings of the Fifth International Symposium on the Controlled Release of Bioactive Materials*, Brinckman, F E and Montemarano, J A (eds), University of Akron Press, Akron (OH, USA), 1978, pp 2.25–2.30
4. Taylor, R T and Hanna, M L *J. Environ. Sci. Health–Environ. Sci. Eng.*, 1976, A11: 201
5. Thayer, J S *J. Environ. Sci Health—Environ. Sci. Eng.*, 1983, A18: 471
6. Thayer, J S *Inorg. Chem.*, 1979, 18: 1171
7. Clark, S and Craig P J, *Appl. Organomet. Chem.*, 1988, 2: (in press)
8. Moore, J W and Pearson, R G *Kinetics and Mechanism*, 3rd Edn, Wiley, New York, 1981, pp 286–288
9. Stone, A T and Morgan, J S *Environ. Sci. Tech.*, 1984, 18: 450
10. Thayer, J S, unpublished observations
11. Thayer, J S *Inorg. Chem.*, 1981, 20: 3573
12. Nexo, E and Olesen, H In: *B_{12}*, Dolphin, D (ed), Wiley, New York, 1982, Vol. 2, pp 57–86
13. Clark, S, Ashby, J and Craig, P J *The Analyst*, Dec. 1987, (in press)

APPENDIX: REACTION PARAMETERS

Nickel(III) oxide

$[CH_3B_{12}]$ (mol dm^{-3}, × 10^5)	Oxide (mmol)	No. of data points	Reaction (%)		k_2(s^{-1}, × 10^3)	k_1(s^{-1}, × 10^4)	(mol dm^{-3}, × 10^5)^7		$A_0/(A_0+B_0)$	r
							A_0	B_0		
1.24	0.470	10	54.8		5.99	6.15	0.11	1.13	0.089	0.994
3.45	1.866	13	65.9		4.76	5.78	0.70	3.15	0.087	0.999
4.96	2.051	7	70.0		5.52	6.05	3.43	1.53	0.692	0.991
5.58	2.070	11	70.0		6.79	7.48	1.70	3.87	0.305	0.992
14.5	0.220	9	75.4		6.52	4.93	7.92	6.30	0.557	0.996
14.9	0.498	17	55.5		5.62	5.78	1.04	13.0	0.074	0.971
15.9	0.205	17	55.1		5.52	5.46	2.14	13.8	0.134	0.998
65.1	0.135	11	50.8		5.83	4.26	6.53	58.6	0.100	0.986
				$\bar{K}$	5.82	5.74				
				S.D.	0.63	0.94				

Nickel(IV) oxide

$[CH_3B_{12}]$ (mol dm^{-3}, × 10^5)	Oxide (mmol)	No. of data points	Reaction (%)		k_2(s^{-1}, × 10^3)	k_1(s^{-1}, × 10^4)	(mol dm^{-3}, × 10^5)^7		$A_0/(A_0+B_0)$	r
							A_0	B_0		
3.36	4.794	13	77.9		3.54	3.99	1.67	1.60	0.511	0.990
3.45	5.580	13	55.3		2.33	2.63	2.33	2.63	0.293	0.990
3.58	4.444	16	60.0		2.40	2.41	1.38	2.32	0.373	0.980
4.68	4.778	13	77.1		2.66	3.10	2.32	2.36	0.496	0.990
5.70	1.821	15	57.7		3.55	3.11	1.25	4.45	0.219	0.990
8.28	4.619	11	60.0		3.83	4.29	1.96	6.32	0.237	0.990
10.3	2.390	15	66.1		2.84	2.56	3.38	6.92	0.328	0.990
				$\bar{K}$	3.13	3.17				
				S.D.	0.62	0.72				

Manganese(IV) oxide

$[CH_3B_{12}]$ (mol dm^{-3}, × 10^5)	Oxide (mmol)	No. of data points	Reaction (%)		k_2(s^{-1}, × 10^6)	k_1(s^{-1}, × 10^7)	(mol dm^{-3}, × 10^5)		$A_0/(A_0+B_0)$	r
							A_0	B_0		
8.00	1.334	7	32.2		7.83	1.25	1.44	6.56	0.180	0.967
8.81	4.836	6	25.8		12.8	1.11	1.35	7.46	0.153	0.992
9.52	6.772	8	21.7		12.5	1.19	1.41	8.11	0.148	0.952
11.3	1.002	10	21.4		7.16	1.07	0.40	10.9	0.035	0.980
13.1	1.975	9	28.4		13.2	1.14	2.80	10.3	0.214	0.950
15.1	4.087	8	22.3		11.7	1.69	2.00	13.1	0.132	0.986
22.3	4.668	6	38.2		7.32	1.14	3.80	17.1	0.182	0.989
24.5	11.896	7	20.3		10.8	0.960	3.70	20.8	0.151	0.969
25.4	7.023	9	26.8		8.00	0.920	4.50	20.9	0.177	0.928
26.9	11.899	9	15.4		9.00	1.22	1.00	25.9	0.037	0.977
43.3	1.150	10	29.6		12.3	1.11	5.00	37.9	0.117	0.971
				$\bar{K}$	10.2	1.15				
				S.D.	2.4	0.19				

Manganese(III) oxide

$[CH_3B_{12}]$ (mol dm^{-3}, × 10^5)	Oxide (mmol)	No. of data points	Reaction (%)		k_2(s^{-1}, × 10^6)	k_1(s^{-1}, × 10^7)	(mol dm^{-3}, × 10^5)^7		$A_0/(A_0+B_0)$	r
							A_0	B_0		
11.3	3.585	11	38.8		8.21	1.59	1.00	10.3	0.088	0.970
16.3	4.491	6	38.6		6.79	1.88	4.00	12.3	0.245	0.984
22.2	2.412	7	49.6		8.27	2.22	5.10	17.1	0.230	0.952
23.1	3.586	12	42.0		8.66	1.87	3.10	20.0	0.134	0.997
23.9	3.140	10	32.2		6.93	1.38	3.10	20.9	0.130	0.988
24.5	9.003	7	30.7		6.84	1.61	5.30	19.2	0.216	0.957
24.6	4.075	8	27.8		6.43	1.28	3.20	21.4	0.130	0.988
63.2	4.301	8	25.1		7.57	1.46	9.50	53.7	0.150	0.982
16.4	3.629	10	33.9		6.56	1.33	1.80	14.6	0.110	0.939
				$\bar{K}$	7.36	1.62				
				S.D.	0.84	0.31				

Manganese(II, III) oxide

$[CH_3B_{12}]$ (mol dm^{-3}, × 10^5)	Oxide (mmol)	No. of data points	Reaction (%)		k_2(s^{-1}, × 10^5)	k_1(s^{-1}, × 10^7)	(mol dm^{-3}, × 10^5)		$A_0/(A_0+B_0)$	r
							A_0	B_0		
6.91	5.389	6	28.0		2.65	1.21	1.45	5.46	0.210	0.993
9.52	3.098	8	36.0		2.42	1.60	2.87	6.65	0.301	0.992
13.1	1.975	7	38.6		2.19	2.29	4.00	9.10	0.305	0.985
13.6	3.628	8	37.5		2.01	2.01	2.60	11.0	0.191	0.958
13.9	4.451	7	39.2		1.90	2.34	3.16	10.7	0.227	0.993
15.1	3.972	7	34.9		1.85	1.81	4.11	11.0	0.272	0.995
19.0	2.309	8	36.5		2.12	2.30	4.60	14.4	0.242	0.994
23.1	2.762	12	40.0		1.54	1.44	4.00	19.1	0.173	0.931
24.5	7.794	7	31.8		1.72	1.92	5.60	18.9	0.229	0.981
				$\bar{K}$	2.04	1.88				
				S.D	0.35	0.40				

Lead(II, IV) oxide (viz. red lead oxide)

$[CH_3B_{12}]$ (mol dm^{-3}, × 10^5)	Oxide (mmol)	No. of data points	Reaction (%)		k_2(s^{-1}, × 10^5)	k_1(s^{-1}, × 10^7)	(mol dm^{-3}, × 10^5)		$A_0/(A_0+B_0)$	r
							A_0	B_0		
4.82	2.079	5	58.8		1.25	6.61	2.28	2.54	0.473	0.941
8.69	1.312	7	61.3		2.13	7.99	3.24	5.45	0.373	0.995
13.6	1.512	6	84.0		2.75	8.3	8.60	5.02	0.632	0.969
23.1	0.866	9	73.7		3.05	8.01	6.30	16.8	0.273	0.996
26.2	1.800	6	70.2		2.42	7.27	12.1	14.2	0.462	0.994
27.4	0.704	7	78.5		2.55	6.63	11.0	16.4	0.401	0.966
				$\bar{K}$	2.36	7.47				
				S.D.	0.62	0.74				

Sodium bismuthate

$[CH_3B_{12}]$ (mol dm^{-3}, $\times 10^5$)	Oxide (mmol)	No. of data points	Reaction (%)		k_2(s^{-1}, $\times 10^4$)	k_1(s^{-1}, $\times 10^6$)	(mol dm^{-3}, $\times 10^5$)		$A_0/(A_0+B_0)$	r
							A_0	B_0		
4.60	0.759	20	24.7		2.67	1.91	1.06	3.86	0.215	0.950
5.25	0.750	16	20.8		3.07	1.59	0.90	4.49	0.167	0.990
5.58	0.720	16	34.0		2.59	2.65	1.13	4.02	0.219	0.960
5.58	0.823	16	27.6		3.15	2.44	0.94	4.58	0.170	0.990
8.69	0.623	6	69.3		3.39	2.07	4.44	4.25	0.511	0.980
8.96	0.361	14	26.2		3.84	2.72	1.01	7.66	0.116	0.980
				$\bar{K}$	3.12	2.23				
				S.D.	0.46	0.46				

Thallium(III) oxide

$[CH_3B_{12}]$ (mol dm^{-3}, $\times 10^5$)	Oxide (mmol)	No. of data points	Reaction (%)		k_2(s^{-1}, $\times 10^3$)	K_1(s^{-1}, $\times 10^4$)	(mol dm^{-3}, $\times 10^5$)		$A_0/(A_0+B_0)$	r
							A_0	B_0		
1.89	1.430	12	55.1		2.12	2.0	0.23	1.66	0.122	0.991
3.52	1.008	13	45.1		1.98	1.0	0.90	2.62	0.256	0.987
3.66	1.353	15	54.7		1.95	1.0	0.74	3.02	0.197	0.998
4.05	1.429	12	37.3		2.33	0.97	0.60	3.45	0.148	0.985
4.46	0.739	10	30.9		3.62	1.1	0.58	3.88	0.129	0.999
4.68	1.032	12	45.2		2.32	1.0	1.11	3.57	0.237	0.991
4.93	1.180	14	49.9		1.34	1.0	1.31	3.62	0.266	0.998
8.28	0.237	9	15.6		2.44	1.8	1.10	7.18	0.133	0.965
8.31	1.905	17	42.1		3.06	0.75	0.97	7.19	0.119	0.998
				$\bar{K}$	2.35	1.27				
				S.D.	0.66	0.44				

Silver(II) oxide

$[CH_3B_{12}]$ (mol dm^{-3}, $\times 10^5$)	Oxide (mmol)	No. of data points	Reaction (%)		k_2(s^{-1}, $\times 10^3$)	k_1(s^{-1}, $\times 10^4$)	(mol dm^{-3}, $\times 10^5$)		$A_0/(A_0+B_0)$	r
							A_0	B_0		
2.52	4.493	11	53.6		3.77	1.83	0.88	1.64	0.349	0.992
3.46	2.979	11	82.9		4.86	2.21	2.62	0.841	0.757	0.998
4.05	3.391	11	55.8		4.29	1.37	1.74	2.31	0.430	0.996
4.68	3.314	11	86.2		4.89	1.95	3.79	0.889	0.757	0.995
5.55	6.953	12	50.1		4.05	1.59	1.81	3.74	0.326	0.994
8.20	4.976	10	86.6		6.47	1.79	6.16	1.33	0.822	0.996
				$\bar{K}$	4.72	1.79				
				S.D.	0.96	0.29				

Silver(I) oxide

$[CH_3B_{12}]$ (mol dm^{-3}, $\times 10^5$)	Oxide (mmol)	No. of data points	Reaction (%)	k_2(s^{-1}, $\times 10^6$)	k_1(s^{-1}, $\times 10^8$)	(mol dm^{-3}, $\times 10^5$)			
						A_0	B_0	$A_0/(A_0+B_0)$	r
13.2	2.430	9	22.4	2.37	1.59	1.4	11.4	0.106	0.988
16.4	2.806	9	14.5	3.83	1.32	1.1	15.3	0.067	0.993
23.3	1.898	11	15.1	3.22	1.13	1.6	21.7	0.069	0.950
23.9	4.321	10	11.5	4.32	1.01	0.8	23.1	0.033	0.990
29.3	2.873	9	29.1	3.28	1.09	2.4	26.9	0.082	0.910
43.3	2.287	10	16.6	2.61	1.15	2.5	40.8	0.058	0.935
			$\bar{K}$	3.27	1.21				
			S.D.	0.73	0.21				